Role of structural relaxations and chemical substitutions on piezoelectric fields and potential lineup in GaN/Al junctions

S. Picozzi, G. Profeta, and A. Continenza
Istituto Nazionale di Fisica della Materia (INFM), Dipartimento di Fisica, Università degli Studi di L'Aquila, 67010 Coppito (L'Aquila), Italy

S. Massidda
Istituto Nazionale di Fisica della Materia (INFM), Dipartimento di Scienze Fisiche, Università degli Studi di Cagliari, 09124 Cagliari, Italy

A. J. Freeman
Department of Physics and Astronomy and Materials Research Center, Northwestern University, Evanston, Illinois 60208
(Received 14 June 2001; revised manuscript received 4 October 2001; published 5 April 2002)

First-principles full-potential linearized augmented plane wave calculations are performed to clarify the role of the interface geometry on piezoelectric fields and potential lineups in [0001] wurtzite and [111]-zincblende GaN/Al junctions. The electric field (polarity and magnitude) is found to be strongly affected by atomic relaxations in the interface region. A procedure is used to evaluate the Schottky-barrier height in the presence of electric fields, showing that their effect is relatively small (a few tenths of an eV). These calculations assess the rectifying behavior of the GaN/Al contact, in agreement with experimental values for the barrier. We disentangle chemical and structural effects on the relevant properties (such as the potential discontinuity and the electric field) by studying unrelaxed ideal nitride/metal systems. Using simple electronegativity arguments, we outline the leading mechanisms that define the values of the electric field and Schottky barrier in these ideal systems. Finally, the transitivity rule is proved to be well satisfied.

DOI: 10.1103/PhysRevB.65.165316 PACS number(s): 73.30.+y, 73.20.−r

I. INTRODUCTION

Wide-bandgap electronic devices are expected to play an important role in the next generation of high-power and high-temperature applications. In particular, extensive work has been carried out in recent years on popular semiconductors such as GaN, AlN, and SiC.[1,2] It is clear, however, that many efforts, theoretical as well as experimental, are still needed to bring the emergent device technology to maturity. Within this context, the GaN/metal interface represents one of the most thoroughly studied topics,[1] but it is not yet clear which are the basic mechanisms leading to the observed behavior—ohmic vs rectifying—of the barrier. A key property of nitrides is the presence of large spontaneous piezoelectric fields, which have to be considered whenever these compounds are used as basic constituents of technological devices.[3] Within the framework of *ab initio* simulations, extensive work has been carried out for nitride/metal contacts, but the GaN structure explored so far has always been zincblende with [001] as the ordering direction.[4] In contrast, most of the experimental work in this field has been focused on the hexagonal wurtzite structure as the stable phase of GaN.[5,6]

In this work, we present results from first-principles calculations using the all-electron full-potential linearized augmented plane wave (FLAPW) method[7] for [0001] wurtzite and [111] zincblende GaN/Al interfaces (denoted *w*-GaN/Al and *z*-GaN/Al, respectively). These systems can be directly compared, since the [111]-ordered zincblende and [0001]-ordered wurtzite structures have the same coordination up to the third nearest-neighbor shell and the interface geometry (in terms of number and direction of bonds) is the same.

II. COMPUTATIONAL DETAILS

The calculations were performed using one of the most accurate first-principles density-functional based methods, namely, the all-electron FLAPW code.[7] Core-level electrons are treated fully relativistically, whereas valence electrons are treated semi-relativistically, i.e., without spin-orbit coupling. Ga $3d$ states are treated as valence electrons, in order to allow their characteristic hybridization with N $1s$ states. The exchange-correlation potential is treated within the local-density approximation, using the Hedin-Lundqvist parametrization.[8] The FLAPW code allows calculation of total energies and atomic forces, so that optimization of the atomic positions is achieved from first principles. The muffin-tin spheres were chosen as $R_{MT}^{Ga}=2.0$ a.u., $R_{MT}^{Al}=2.0$ a.u., and $R_{MT}^{N}=1.6$ a.u., and the expansion in spherical harmonics in these regions was performed up to $l\leqslant 8$; in the interstitial part, a cut-off for the wave functions $k_{max}=4.0$ a.u.$^{-1}$ was used. The Brillouin-zone sampling was done according to the Monkhorst-Pack scheme,[9] using ten **k** points in the irreducible part of the zone.

The supercell employed corresponds to six layers of GaN (i.e., seven N and six Ga layers) and six layers of Al, with a total of 19 layers per cell. Calculations performed with varying cell dimensions have shown that this particular choice of number of layers is sufficient to recover the proper bulk conditions away from the interface; this is a major requirement

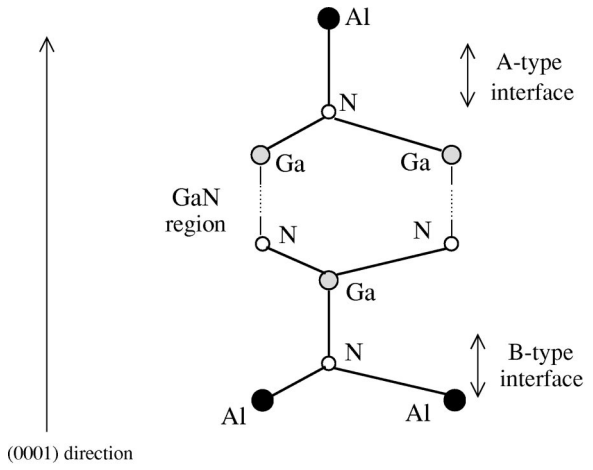

FIG. 1. *A*- and *B*-type interface geometries.

when dealing with potential lineup problems within the supercell approach.

The equilibrium atomic-force- and total-energy-optimized *w*-GaN lattice parameters are $a=3.16$ Å and $c=1.624a$ with an internal parameter $u=0.377$; for the zincblende structure we find $a=4.48$ Å. The agreement with the experimental values ($a=3.16$ Å, $c/a=1.62$, and $u=0.377$ for wurtzite, and $a=4.48$ Å for zincblende)[10] is excellent, as is usual for FLAPW structural results for III-V semiconductors.

III. STRUCTURES AND ENERGETICS

A. Relaxed GaN/Al junctions

Optimization of atomic positions is relevant in the GaN/Al system. As shown for [001] *z*-GaN/Al,[4] the Schottky-barrier height (SBH) is very sensitive to the interface geometry, namely, to the interplanar distances in proximity of the junction. Due to the polar nature of the interface in the systems of interest here, we expect an even stronger effect of the structural configuration. In fact, for both [0001] *w*-GaN/Al and [111] *z*-GaN/Al, two inequivalent N-terminated interfaces are possible. As shown in Fig. 1, in *A*-type interfaces, N is bonded to three Ga and one Al with the ''long'' Al-N bond parallel to the growth axis; in *B*-type interfaces, N is bonded to three Al and one Ga, leading to an interplanar distance that is ideally one third of the bond length.

All the atomic positions were allowed to relax; the relevant interface bond lengths for the optimized geometries are shown in Table I. First of all, we note that the differences in bond lengths between zincblende and wurtzite systems are very small (less than 0.1%); this indicates the similarity of the [111] *z*-GaN/Al and [0001] *w*-GaN/Al junctions. The interfacial Ga-N distances can be compared with the bulk *w*-GaN bond length of 1.92 Å; they are found to differ by only 1%, showing that the relaxations in the semiconductor side are rather small. As expected, only the *interface* bond lengths in the semiconductor side deviate slightly from the bulk distances; already in the second layer, the first-nearest-neighbor bond lengths typical of bulk *w*-GaN are recovered (within 0.3%). On the contrary, the Al-Al bond lengths in the metallic layer deviate by as much as 10% from the calculated Al-Al interplanar distance in fcc-Al (111) strained on *w*-GaN (0001) ($z_{Al\text{-}Al}=2.046$ Å). We find some bigger differences between the relaxations in the two inequivalent interfaces, mainly in the Al-N bond length. In *B*-type interfaces, the Al-N bond length is more or less unaltered (by $<0.4\%$) with respect to the bulk Ga-N bond length, so that Al perfectly replaces the Ga cation of bulk GaN. On the other hand, in *A*-type interfaces the Al-N bond length is smaller (by 2.2%) than the bulk Ga-N bond length, and much closer to the bulk *w*-AlN bond length ($d_{Al\text{-}N}^{w\text{-}bulk}=1.87$ Å).[10] That is, the tendency of Al and N atoms to get closer is higher (lower) when they are aligned (not aligned) along the growth direction.

TABLE I. Interface bond lengths (in Å) in the fully relaxed systems at the *A*- and *B*-type interfaces (see text and Fig. 1).

	$(w\text{-GaN/Al})^{rel}$		$(z\text{-GaN/Al})^{rel}$	
	A type	*B* type	*A* type	*B* type
d_{GaN}	1.94	1.95	1.94	1.94
d_{AlN}	1.89	1.93	1.89	1.93

B. Unrelaxed and partially relaxed GaN/Al junctions

In order to further investigate the effect of relaxations, we also considered unrelaxed and partially relaxed systems. The ''ideal'' (i.e., unrelaxed) system, denoted as $(w\text{-GaN/Al})^{id}$, is obtained from [0001]-ordered bulk *w*-GaN, by removing the N atoms and substituting the Ga atoms for Al in half of the material. This gives rise to a *w*-GaN/Al junction with Ga-N and Al-N interface distances equal to the Ga-N distances in *w*-GaN, and Al-Al distances matching the distance between Ga cations in *w*-GaN. In the ''partially relaxed'' system, denoted as $(w\text{-GaN/Al})^{pr}$, all the interface and subinterface interplanar distances in the semiconductor side are those of the relaxed system, and the Al-Al distances in the metal side are forced to be the same.

We focus first on the stability of the different systems. We show in Table II the energy gain per atom of each system, referred to the most stable system, i.e., $(w\text{-GaN/Al})^{rel}$. We observe that the effect of atomic relaxations in the interface region is quite high—about 50 meV/atom of energy gain difference between $(w\text{-GaN/Al})^{id}$ to $(w\text{-GaN/Al})^{pr}$—despite the fact that their bulk bond lengths differ by less than 2%. On the other hand, the energy is very stable against atomic relaxation in the bulk Al; it varies by only 6 meV/atom. As expected, the interface geometry in the semiconductor side is critical, while changes of the atomic positions within the bulk metal region are far less energetically expensive. Also, in agreement with previous results,[11] we found that the zincblende structure is not favored compared to the wurtzite phase (but only by at most 10 meV/atom).[12]

In order to separate *chemical* and *structural* contributions to the SBH, we considered some unrelaxed [111]-ordered $(z\text{-}X\text{N}/Y)^{id}$ systems, where $X,Y=$Ga,Al. In these junctions, the atomic positions are frozen and set equal; only the chemical species occupying the atomic sites differ. More-

TABLE II. Energy gain per atom (in meV/atom) of the different systems referred to $(w\text{-GaN/Al})^{rel}$. The estimated error is about 2 meV/atom.

$(w\text{-GaN/Al})^{rel}$	$(z\text{-GaN/Al})^{rel}$	$(w\text{-GaN/Al})^{pr}$	$(w\text{-GaN/Al})^{id}$	$(z\text{-GaN/Al})^{id}$
0	10	6	55	59

over, the zincblende undistorted structure does not show any spontaneous piezoelectric field because of symmetry. These model nitride/metal junctions are not meant to simulate real systems; in fact, since the stable structure of Ga is the complex α-Ga structure, interface relaxations and coordinations in the real *X*N/Ga junctions could be completely different from those considered here. Nevertheless, we will take these ideal systems as reference structures.

Insights into the chemical bonding at the nitride/metal interfaces can be gained by focusing on the adhesion energy, E_{ad}.[13] In order to estimate the gain in energy when depositing Al or Ga on a nitride surface, we calculated the difference between the adhesion energies in the $(X\text{N/Ga})^{id}$ and $(X\text{N/Al})^{id}$ junctions: $E_{ad}(\text{GaN/Al})^{id} - E_{ad}(\text{GaN/Ga})^{id} = 1.04$ eV and $E_{ad}(\text{AlN/Al})^{id} - E_{ad}(\text{AlN/Ga})^{id} = 1.06$ eV. The larger energy gain for deposition of Al versus Ga on the N-terminated nitride surface is in agreement with the larger formation energy of the Al-N bond compared to Ga-N.[14] Moreover, the gain in adhesion energy is similar for the two nitride surfaces.

C. Other model systems: Unrelaxed *z-XN/Y/X* (*X,Y*=Ga, Al)

Finally, to investigate the role of a single metallic interlayer on the SBH and electric field, we also focused on two systems, $(z\text{-AlN/Ga/Al})^{id}$ and $(z\text{-GaN/Al/Ga})^{id}$. These systems are obtained from the ideal $(z\text{-}X\text{N}/X)^{id}$ junction by substituting the first *X* monolayer of the metallic side for a *Y* monolayer.

IV. DENSITY OF STATES

Let us investigate the two inequivalent interfaces (*A* and *B* in Fig. 1) in terms of their density of states for wurtzite-based systems (zincblende-based systems are very similar and therefore not discussed). In Fig. 2, we show the projected density of states (PDOS) on the Ga, N, and Al interface atomic planes of the relaxed *w*-GaN/Al junction for *A*-type [Figs. 2(a)–2(c)], and *B*-type [Figs. 2(d)–2(f)] interfaces. Figures 2(a) and 2(d) show that the interface Ga atomic plane in both the *A*- and *B*-type junctions has a PDOS very similar to that of the Ga atomic plane in bulk *w*-GaN, except for the increased DOS near E_F due to metal-induced gap states. On the other hand, the PDOS at the interface N atomic plane clearly differs in the *A*- and *B*-type junctions; note, in particular, that the feature at -8 eV in Fig. 2(b), mainly due to cation *s* states, is shifted towards smaller binding energies (to about -7 eV) in Fig. 2(e). A more careful investigation shows that many of the interface N PDOS features for *A*-type junctions are common to bulk *w*-GaN [see dashed line in Fig. 2(b)], while the interface N PDOS for *B*-type junctions is more similar to the one in bulk *w*-AlN [dashed line in Fig. 2(e)]. A simple rationale can be found by considering the geometry of the two inequivalent interfaces shown in Fig. 1. In *A*-type junctions, the four N sp^3 orbitals point towards three Ga and one Al, whereas they point towards three Al and one Ga in *B*-type junctions. Thus, we expect the behavior of interface N atoms in GaN/Al to be similar to that in bulk *w*-GaN (*w*-AlN) for the *A*- type (*B*-type) interfaces.

The interface Al PDOS is remarkably different in the two inequivalent junctions. In terms of PDOS, *B*-type interface Al resembles Al in bulk *w*-AlN [dashed line in Fig. 2(f)], whereas *A*-type interface Al shows a free-electron-like behavior, close to the one in bulk fcc-Al [dashed line in Fig. 2(c)]. The metallicity of the interface Al plane in *A*-type junctions is confirmed by the nonzero DOS in the band-gap region (i.e., from about -2 eV to the Fermi level, E_F). The higher interface Al PDOS at E_F for *A*-type junctions [Fig. 2(c)] suggests a more effective screening for *B*-type interfaces [Fig. 2(f)].

Finally, the bond length does not greatly affect the DOS. In fact, the PDOS (not shown) for the ''frozen'' reference structure $(w\text{-GaN/Al})^{id}$, having interface AlN and GaN bond distances equal to those in bulk *w*-GaN, is very similar to the PDOS for the relaxed system, where interface AlN and GaN bond distances are different from bulk. Therefore, the electronic behavior is dictated by the number and direction of bonds between different atoms rather than by their length.

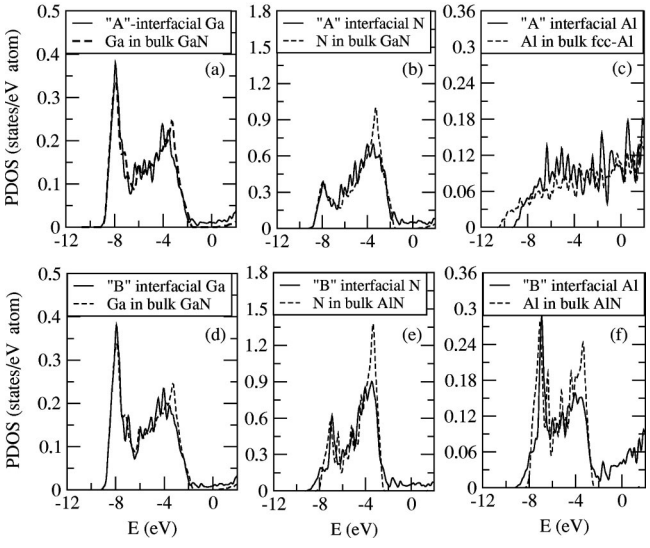

FIG. 2. Density of states (states/eV atom) projected on the interface Ga [panels (a) and (d)], N [panels (b) and (e)], and Al [panels (c) and (f)] planes for *A*- and *B*-type $(w\text{-GaN/Al})^{rel}$ junctions, respectively.

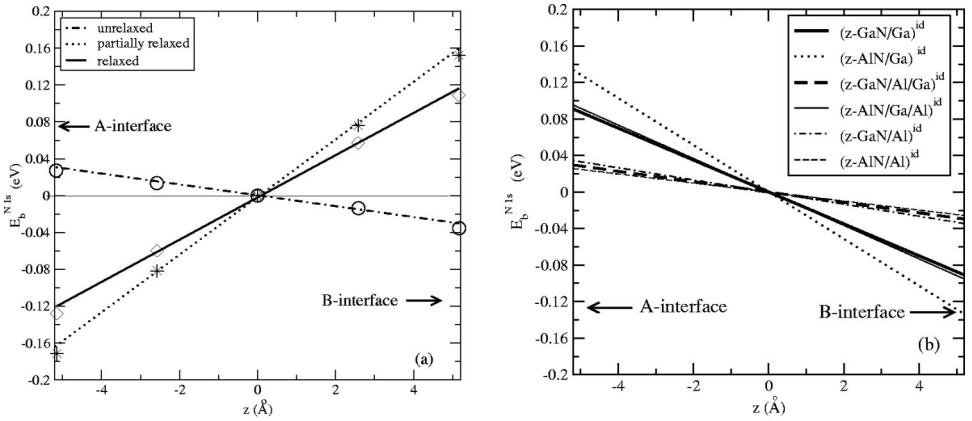

FIG. 3. Panel (a): N 1s core-level binding energy (in eV) vs z coordinate along the growth axis (in Å), in the semiconductor bulk region, for ideal (circles), partially relaxed (stars), and relaxed (diamonds) GaN/Al junctions. Panel (b): linear fit of the N 1s core-level binding energy (in eV) vs z coordinate (in Å), for XN/Y and XN/Y/X ideal systems (X,Y = Ga,Al).

V. ELECTRIC FIELDS

The inequivalency of *A*-type and *B*-type interfaces, in terms of geometry and bond lengths, gives rise to electric fields. In addition, in wurtzite-based systems we expect the presence of spontaneous piezoelectric fields, which vanish by symmetry in zincblende-based junctions. The N 1*s* core-level binding energies in wurtzite-based systems for ideal, partially and fully relaxed systems vary linearly with depth, as shown in Fig. 3(a). The binding-energy scale has been shifted so that the binding energy at the center of the GaN region is zero. The slope of the linear dependence gives the electric field; its magnitude is listed in Table III for all the systems examined. The interface regions have been excluded, because they are subjected to local effects, due to charge rearrangement in proximity of the junction. We expect the polarization charge, giving rise to the electric field, to be strongly affected by the interface geometry; in fact, the polarity of the field changes in going from ideal to relaxed systems [see Fig. 3(a)].

The mechanisms giving rise to the electric field are very complicated; it results from the interplay of boundary conditions, interface charge redistribution, and screening effects. The value and even the polarity of the field cannot be determined using simple electrostatic or electronegativity arguments. In this context, *ab initio* simulations are the only way to take into account the microscopic details of the charge rearrangement and the boundary conditions, giving a correct description of the overall electrostatics. It can be argued that the almost negligible electric field present in the unrelaxed system is due to the tendency of Al to screen the electric field; this is undoubtedly true for every good metal. However, the large total energy difference between ideal and relaxed systems (see Table II) suggests that the electrostatic energy accumulated in the semiconductor side by the field is negligible by far, compared to other energy terms related to structural relaxations. Furthermore, the difference between the values of the electric field in zincblende and wurtzite systems is quite small, so that the presence of intrinsic piezoelectric fields is not playing a significant role in the determination of the potential lineup (see below).

The N 1*s* core-level binding energy for unrelaxed zincblende systems is shown in Fig. 3(b). The polarity of the electric field is the same in all the ideal systems but the magnitude shows large variations. It could be argued, on the basis of Fig. 3(b), that more symmetric junctions (i.e., with similar anion-cation bond lengths at the two sides of the interface) would exhibit smaller fields. Nevertheless, Fig. 3(b) shows a large spread of electric field magnitudes, even though all the systems considered are ideal symmetric junctions. This shows the complexity of the problem, with the interplay of structural and chemical effects. We can give a rationale to a part of the observed behavior. For example, we note that in all ideal systems having Al (Ga) next to the interface, the electric field is negligible (quite large); it seems that interfacial Al favors charge rearrangement in such a way as to screen the electric field much more efficiently than Ga. As for the comparison between the two different nitrides, we expect, on the basis of ionicity arguments, a larger interface bond charge for AlN than for GaN; this is confirmed by most of the results shown in Fig. 3(b).

Let us consider the (z-GaN/Ga)^{id} and (z-GaN/Al/Ga)^{id} systems. The only difference between these two systems is the metal layer next to N; however, the corresponding electric fields are very different [see Fig. 3(b)]. This shows that

TABLE III. Electric fields (in mV/Å) and Schottky-barrier heights (in eV) at the two inequivalent *A*- and *B*-type interfaces. The positive sign for the electric field values is assigned taking into account that the core levels are deeper in going from *B*- to *A*-type interface. The estimated error is about 0.5 mV/Å.

	(w-GaN/Al)^{rel}	(z-GaN/Al)^{rel}	(w-GaN/Al)^{pr}	(w-GaN/Al)^{id}	(z-GaN/Al)^{id}
E	23	14	31	−5	−7
Φ^A	2.07	1.98	1.99	1.84	1.69
Φ^B	1.69	1.76	1.48	1.93	1.80

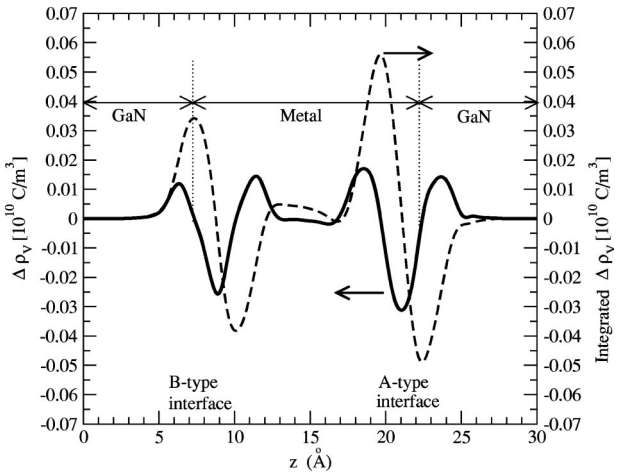

FIG. 4. Difference between the macroscopic planar average of the valence charge densities in $(z\text{-GaN/Ga})^{id}$ and $(z\text{-GaN/Al/Ga})^{id}$ as a function of depth (solid line). Also shown is its integral (dashed line).

the major role in establishing the field is played by the interface metal layer, rather than by the screening properties of the metal side of the junction. In other terms, the electric field, for fixed periodic boundary conditions, is determined by ''interface'' effects rather than by ''bulk'' properties of the constituents. In order to clarify the role of the interface metal layer, we plot in Fig. 4 the difference between the double macroscopic average[15] of the valence charge densities for $(z\text{-GaN/Ga})^{id}$ and $(z\text{-GaN/Al/Ga})^{id}$ systems. The solid line in Fig. 4 demonstrates the different ionic character of AlN and GaN: more charge is localized at the interface N layer when N is bonded to Al than to Ga. Moreover, the charge difference integral (dashed line in Fig. 4) shows that this effect is more pronounced for *A*-type interfaces, where the metal-N bond is parallel to the growth axis. This is in agreement with what was above pointed out for the relaxed $(\text{GaN/Al})^{rel}$ systems: due to the particular interface geometry, charge transfer from Al to N is favored in *A*-type junctions compared to *B*-type ones.

Finally, we observe that the effect of the Ga *d* electrons on the electric field is negligible. In fact, if we consider the $(z\text{-GaN/Ga})^{id}$ system and treat the Ga *d* states as valence or core electrons, we obtain exactly the same electric field.

VI. SCHOTTKY-BARRIER HEIGHTS

Let us now discuss the most technologically important property, the Schottky-barrier height and its relation to piezoelectric fields. Usually, within all-electron methods the SBH is evaluated following a procedure based on core-level energies taken as reference.[16] The SBH is expressed as

$$\Phi = \Delta b + \Delta E_b , \tag{1}$$

where Δb is the difference between the Ga and Al $1s$ core-level energies far from the junction, and is typically an interface contribution. ΔE_b, on the other hand, is a bulk contribution and is given by the difference between the semiconductor Ga $1s$ binding energy with respect to the valence-band maximum and the metal Al $1s$ binding energy with respect to E_F: $\Delta E_b = (E^{GaN}_{VBM} - E_{Ga1s}) - (E^{Al}_{Fermi} - E_{Al1s})$. However, evaluation of the barrier height in the presence of electric fields is not straightforward and deserves an appropriate discussion. In fact, whenever an electric field is present in the semiconductor side, the core-level binding energies (or equivalently the electrostatic potential) depend on the position *z*, so that Eq. (1) is ill defined.

We therefore considered a linear extrapolation of the core-level binding energies (or of the macroscopic average of the electrostatic potential) and take for the reference energies used in Eq. (1) the values extrapolated at the two interface planes (defined in the next paragraph). We then added up the value of the binding energy in the semiconductor side and obtained two values, whose distance from E_F gives the SBH. In this way, we implicitly assume that the Fermi level of the system is fixed to the one in the metal side. This procedure is equivalent to that based on the PDOS on the different atomic layers, where the SBH is obtained from the difference between the valence-band maximum in the bulk semiconductor and the Fermi level. Previous studies[4] show that the results so obtained agree with those obtained from Eq. (1) within 0.1–0.2 eV.

Let us define the interface plane for *A*- and *B*-type junctions. From the depth dependence of the double macroscopic average of the valence charge density (not shown) we find that the interface dipole, defining the potential lineup, is centered in the interfacial N layer for *B*-type junctions, and halfway between interface Al and N planes for *A*-type junctions. The plane where the interface dipole is centered is arbitrarily defined as the interface plane. We kept this choice for all our analyzed structures since the dipole location does not change for the different systems. We can estimate the uncertainty related to this arbitrary choice, by considering interface planes that coincide with the extremes of the interface region, namely, the interface Al and N planes. This leads to an energy difference of the order of a few hundredths of an eV (<0.06 eV), so that the overall uncertainty in the SBH values adds up to 0.15 eV (including also the uncertainties in core-level binding energies and position of E_F).

Since the supercell approach employed introduces artificially two different interfaces (*A* and *B* in Fig. 1) and therefore spurious boundary conditions, it is worthwhile exploring whether this unrealistic model is reliable for SBH evaluation, or instead gives a SBH dependent value on the boundary conditions. To clarify this point we considered a larger *w*-GaN/Al system consisting of 17 GaN (9 N and 8 Ga) and 6 Al layers, with the same interface configuration (i.e., the same interplanar distances in proximity of the junction) as that previously considered. As shown in Fig. 5, we find that the calculated electric field is stronger (or, equivalently, the potential has a steeper slope) for the smaller system; however, the SBH remains constant. This shows that the conserved property of the system is the SBH; the electric field modifies accordingly, fulfilling the boundary conditions and keeping constant the difference between the SBHs at the two inequivalent interfaces. Hence, the procedure used to estimate the potential lineup is correct.

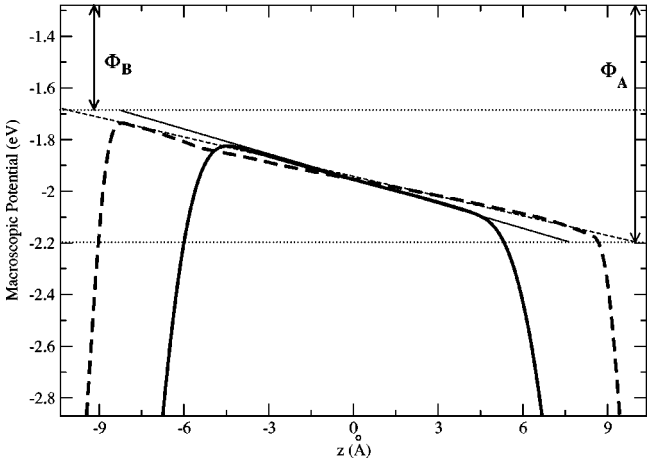

FIG. 5. Macroscopic planar average of the electrostatic potential (in eV) as a function of depth in the GaN region of $(w\text{-GaN/Al})^{rel}$ junctions: comparison between the calculations for cells corresponding to 13 GaN layers (seven N and six Ga layers), thick solid line, and 17 GaN layers (nine N and eight Ga lyers), thick dashed line. The thin solid (dashed) line marks the slope (electric field) for the smaller (bigger) cell size.

Let us now discuss the values of the SBH estimated for the relaxed and partially relaxed systems (see Table III); quasiparticle effects and spin-orbit coupling have been neglected. First of all, note that, within the procedure used to estimate the SBH, the difference between the Schottky-barrier heights at the inequivalent interfaces ($\Delta\Phi^{A\text{-}B}$) is given by the electric field times the thickness of the semiconductor region (potential drop across the semiconductor). This implies that, for infinite thickness, the electric field tends to vanish, so as to maintain a finite $\Delta\Phi^{A\text{-}B}$. This is consistent with the different charge rearrangement occurring at each interface type, so that the Schottky-barrier height at a certain interface is a well defined quantity, not dependent on boundary conditions.[17] Within the uncertainty estimated above, we observe that all SBH values are in the range 1.5–2.0 eV (see Table III). Due to the electric field, the barrier is generally higher in *A* type than in *B* type interfaces for relaxed systems. A straightforward comparison of the Schottky barriers calculated here with the value for cubic [001] *z*-GaN/Al (1.51 eV)[4] cannot be done because the interface morphology is very different. In terms of bond lengths and interface geometry, we find stronger similarities of this system with *B*-type relaxed interfaces, whose SBH comes out to be very close to the one in [001] *z*-GaN/Al.

From the experimental point of view, the transport properties of the GaN/Al junction are still under debate. As for the nature of the contact, it seems well established that unannealed junctions show a rectifying behavior;[6,14,18,19] however, many different values for the SBH exist in the recent literature. For example, photoemission measurements for the [0001] *p*-doped *w*-GaN/Al junction indicate a barrier value of 0.8 eV or 1.5 eV,[14,6] whereas current-voltage characteristics suggest a barrier of 0.6 eV.[19] Our results (see Table III) agree with the rectifying behavior experimentally found; our values are in quantitative agreement with the photoemission results by Bermudez *et al.*[6] Nevertheless, it has to be pointed out that complex chemical reactions occur at the interface: the much larger heat of formation of AlN compared to GaN (Ref. 14) drives a Ga-Al interface exchange reaction, so that the junction becomes a metal-insulator-semiconductor Al/AlN/GaN structure. Moreover, since several kinds of defects and impurities (such as oxygen and N vacancies) have been reported to occur at the interface,[14,18,19] the theoretical and experimental values of the SBH cannot be directly compared.

TABLE IV. Electric fields (in mV/Å) and Schottky-barrier heights (in eV) in *A*- and *B*-type unrelaxed junctions.

	E	Φ^A	Φ^B
$(z\text{-GaN/Al})^{id}$	−7	1.69	1.80
$(z\text{-GaN/Ga})^{id}$	−17	1.67	1.95
$(z\text{-GaN/Al/Ga})^{id}$	−5	1.91	2.00
$(z\text{-AlN/Ga})^{id}$	−25	2.42	2.84
$(z\text{-AlN/Al})^{id}$	−5	2.47	2.55
$(z\text{-AlN/Ga/Al})^{id}$	−18	2.40	2.70

Finally, in order to disentangle structural from chemical contributions to the SBH, let us discuss the barrier values calculated for ideal systems in relation to the corresponding electric fields (see Table IV). First of all, SBHs for $(\mathrm{GaN}/Y)^{id}$ $(Y=\mathrm{Ga, Al})$ interfaces are generally smaller (1.7–2.0 eV) than for $(\mathrm{AlN}/Y)^{id}$ (2.4–2.8 eV). The rectifying behavior of the contact is therefore stronger for the more ionic AlN than for GaN. On the other hand, for different metals on a given semiconductor, we note slightly smaller modifications of the barrier (within 0.3 eV). Furthermore, we find that the difference between the SBHs in *A*- and *B*-type interfaces is smaller for Al than for Ga contacts. This is consistent with the smaller electric field found for Al contacts, and with the more effective screening properties of Al discussed above.

Consider now the effect of the metallic intralayer on the barrier. Any difference in SBH for $X\mathrm{N}/X$ junctions with and without an intralayer has to be ascribed to the interface term, Δb, since the bulk term, ΔE_b, is the same. The overall effect is quite small (0.2 eV at most) and the type of metallic layer is not important for the SBH value, as long as the interface geometry is kept constant.

Finally, it is interesting to check the transitivity rule[15] for the potential lineup in these ideal systems with inequivalent interfaces. In our case, each junction (*A*- or *B*-type) can be thought as being composed of different stacked junctions:

$$(X\mathrm{N}/Y)^{id}_A=(X\mathrm{N}/X)^{id}_A+(X/Y\mathrm{N})^{id}_B+(Y\mathrm{N}/Y)^{id}_A,$$

$$(X\mathrm{N}/Y)^{id}_B=(X\mathrm{N}/X)^{id}_B+(X/Y\mathrm{N})^{id}_A+(Y\mathrm{N}/Y)^{id}_B.$$

The transitivity rule is expressed as:

$$\Phi^A(X\mathrm{N}/Y)=\Phi^A(X\mathrm{N}/X)-\Phi^B(Y\mathrm{N}/X)+\Phi^A(Y\mathrm{N}/Y).$$

From our calculations $\Phi^A(\mathrm{AlN/Ga})=2.42$ eV and $\Phi^B(\mathrm{AlN/Ga})=2.84$ eV. According to the transitivity rule:

$$\Phi^A(\mathrm{AlN/Al}) - \Phi^B(\mathrm{GaN/Al}) + \Phi^A(\mathrm{GaN/Ga})$$
$$= 2.47 - 1.80 + 1.67 = 2.34 \ \mathrm{eV},$$

$$\Phi^B(\mathrm{AlN/Al}) - \Phi^A(\mathrm{GaN/Al}) + \Phi^B(\mathrm{GaN/Ga})$$
$$= 2.55 - 1.69 + 1.95 = 2.81 \ \mathrm{eV}.$$

Thus, there is good agreement with the calculated Φ^A(AlN/Ga) and Φ^B(AlN/Ga) values (within the uncertainty of the calculations), and the transitivity rule is well satisfied. This result shows the reliability of the method proposed here to evaluate SBHs.

VII. CONCLUSIONS

We have performed *ab initio* FLAPW calculations of the potential lineup at GaN/Al interfaces, for both [111]-oriented zincblende and [0001]-oriented wurtzite systems. Our calculations focused on the effects of structural modifications on total energies, electric fields, and SBHs. We have shown that, as expected, the interface geometry is very important; for example, relaxation of the interface Al atomic positions can even reverse the polarity of the electric field. The value of the electric field is the result of a complicated interplay between boundary conditions, charge rearrangement at the junction, and screening effects, and cannot be simply given on the basis of electronegativity arguments or bond configuration at the interface. However, we have identified some leading mechanisms in establishing the electric field in ideal unrelaxed systems, related to the different chemical species in the nitride and metallic sides of the junction.

On the other hand, the SBH for a fixed geometry is independent of boundary conditions.

Our procedure to estimate the SBH in the presence of an electric field is found to give reliable results, reproducible when increasing the unit-cell dimensions. We have shown that the value of the SBH is not greatly affected by the presence of electric fields, of whatever polarity; this leads to changes in the SBH of only a few tenths of an eV. Good agreement with available experimental data is also found. Finally, the transitivity rule was tested for ideal systems with *A*- and *B*-type interfaces; it provides SBH values in excellent agreement with the calculated values, showing the consistency of our calculations.

ACKNOWLEDGMENTS

We acknowledge useful discussions with Dr. F. Bernardini and Dr. P. Ruggerone. This work was supported by the U.S. National Science Foundation (through the Materials Research Center at Northwestern University).

[1] See,for example, P. Kung and M. Razeghi, Opto-Electron. Rev. **8**, 201 (2000), Solid-State Electron. **42**, 677 (1998).
[2] P. Ferrara, N. Binggeli, and A. Baldereschi, Phys. Rev. B **55**, R7418 (1997).
[3] F. Bernardini and V. Fiorentini, Appl. Surf. Sci. **166**, 23 (2000); A. Di Carlo, F. Della Sala, P. Lugli, V. Fiorentini, and F. Bernardini, Appl. Phys. Lett. **76**, 3950 (2000).
[4] S. Picozzi, A. Continenza, G. Satta, S. Massidda, and A.J. Freeman, Phys. Rev. B **61**, 16 736 (2000); S. Picozzi, A. Continenza, S. Massidda, A.J. Freeman, and N. Newman, *ibid.* **58**, 7906 (1998).
[5] U. Karrer, O. Ambacher, and M. Stutzmann, Appl. Phys. Lett. **77**, 2012 (2000).
[6] V.M. Bermudez, T.M. Jung, K. Doverspike, and A.E. Wickenden, J. Appl. Phys. **79**, 110 (1996).
[7] E. Wimmer, H. Krakauer, M. Weinert, and A.J. Freeman, Phys. Rev. B **24**, 864 (1981); H.J.F. Jansen and A.J. Freeman, *ibid.* **30**, 561 (1984) and references therein.
[8] L. Hedin and B.I. Lundqvist, J. Phys. C **4**, 2062 (1971).
[9] H.J. Monkhorst and J.D. Pack, Phys. Rev. B **13**, 5188 (1976).
[10] *Numerical Data and Functional Relationships in Science and Technology*, edited by K. H. Hellwege, Landolt-Börnstein Tables, Group III, Vol. 17a (Springer, New York, 1982).
[11] C.Y. Yeh, S.H. Wei, and A. Zunger, Phys. Rev. B **50**, 2715 (1994).
[12] This is consistent with the observed possibility of epitaxially growing cubic instead of hexagonal GaN under specific conditions.
[13] As usual, the adhesion energy is defined following R. Stadler, D. Vogtenhuber, and R. Podloucky, Phys. Rev. B **60**, 17 112 (1999) and references therein.
[14] C.I. Wu and A. Kahn, J. Vac. Sci. Technol. B **16**, 2218 (1998).
[15] S. Baroni, R. Resta, A. Baldereschi, and M. Peressi, in *Spectroscopy of Semiconductor Microstructures*, edited by G. Fasol, A. Fasolino and P. Lugli (Plenum, New York, 1989), p. 251.
[16] S. Massidda, B.I. Min, and A.J. Freeman, Phys. Rev. B **35**, 9871 (1987).
[17] A. Ruini, R. Resta, and S. Baroni, Phys. Rev. B **57**, 5742 (1998); and **56**, 14 921 (1997).
[18] Z.M. Zhao, R.L. Jiang, P. Chen, W.P. Li, D.J. Xi, S.Y. Xie, B. Shen, and R. Zhang, Appl. Phys. Lett. **77**, 3140 (2000).
[19] C.I. Wu, A. Kahn, A.E. Wickenden, D. Koleske, and R.L. Henry, J. Appl. Phys. **89**, 425 (2001).